



# Thermal influence of boundaries on the onset of Rayleigh–Bénard convection

P. Cerisier<sup>a\*</sup>, S. Rahal<sup>a</sup>, J. Cordonnier<sup>a</sup>, G. Lebon<sup>b</sup>

<sup>a</sup>*IUSTI, UMR CNRS 6595, University of Provence, 13453, Marseille Cedex 13, France*

<sup>b</sup>*Thermo-Mécanique, University of Liège, Sart Tilman, 4000 Liège, Belgium*

Received 26 July 1996; in final form 2 October 1997

## Abstract

The Bubnov–Galerkin method was applied to the problem of onset of convection in a horizontally infinite liquid layer set between two blocks with different thermal conductivities and thicknesses. The critical Rayleigh number ( $Ra_c$ ) and wavenumber ( $k_c$ ) were determined for a range of conductivities and thicknesses. Computations, based on the finite element method, for the steady conductive regime (motionless liquid) suggest that lateral walls, with different thermal admittances appropriate to a finite vessel, have no appreciable effect on  $Ra_c$  and  $k_c$  when the aspect ratio is larger than two. Values calculated from the theoretical model are in reasonable agreement with experimental results. © 1998 Elsevier Science Ltd. All rights reserved.

## Nomenclature

$d$  depth of the liquid layer  
 $d_i$  thickness of the limiting horizontal plate  $i$   
 $D$  differential operator  $d/dz$   
 $g$  gravity  
 $k$  wavenumber  
 $r_i = \lambda/\lambda_i$  ratio of thermal conductivities  
 $Ra$  Rayleigh number  
 $T_m$  mean temperature of the liquid  
 $T_\infty$  temperature of the atmosphere  
 $TIL$  thermal influence length  
 $V$  velocity perturbation  
 $VE_i$  vessel made of material  $i$   
 $u, v, w$  velocity components in  $x, y, z$  directions  
 $x, y, z$  spatial Cartesian coordinates.

## Greek symbols

$\alpha$  coefficient of thermal expansion of the liquid  
 $\Gamma_i$  aspect ratio of the vessel in the  $i$  direction  
 $\delta_i = d_i/d$  ratio of thickness  
 $\delta T$  temperature difference between the limiting horizontal surfaces  
 $\Delta$  Laplacian operator

$\Theta$  temperature perturbation  
 $\kappa$  thermal diffusion of the liquid  
 $\lambda$  thermal conductivity of the liquid  
 $\lambda_i$  thermal conductivity of the horizontal boundary  $i$   
 $\nu$  kinematic viscosity of the liquid.

## Subscripts

$c$  critical value  
 $l$  lower surface  
 $m$  mean  
 $u$  upper surface.

## 1. Introduction

During the last decades the Bénard problem has received great attention as the canonical example of a dissipative structure exhibiting successively ordered, disordered pattern and the phenomena of turbulence, with particular simplicity.

In theoretical considerations, the most usual situation is that of a fluid layer, infinitely extended in the horizontal direction, but limited by two horizontal planes at fixed temperatures. Although the first experimental studies started with the turn of this century [1] and the theoretical ones a little later [2], the first really precise neutral stability curves were proposed by Reid and Harris [3]. In

\* Corresponding author.

the first calculations, the horizontal limiting surfaces are supposed perfect heat conductors at fixed temperatures. This condition is experimentally achieved when the fluid has a low thermal conductivity compared to that of horizontal limiting blocks. Such conditions occur for instance in a layer of water between copper plates. The conductivity ratio of copper and water lies in the order of 500. In such conditions, the temperature disturbances vanish and the temperature of the boundaries remain uniform. For a laterally-infinite fluid layer confined between fixed horizontal boundaries of high thermal conductivity, the critical Rayleigh number for onset of convection is  $Ra_c = 1708$  [4]. These predictions have been verified in the laboratory [5].

But in many problems encountered in nature, industries or laboratories, boundaries cannot be assumed to be good heat conductors. Therefore, more general boundary conditions for temperatures must be used. The temperature disturbances penetrate the walls. The heat flux and the temperatures obey the continuity equation on the boundaries. So it is necessary to consider the influence of the ratios  $r_i = \lambda/\lambda_i$  of thermal conductivity of the liquid to that of boundaries ( $i = u, l$  where  $u$  and  $l$  stand, respectively, for the upper and the lower blocks). Jeffreys [6] was the first to take into account the influence of  $r$  upon the critical Rayleigh number  $Ra_c$ . An analysis was performed by Sani [7] and Sparrow et al. [8]. They studied the stability problem, in which the heat transfer on the boundaries satisfies a linear Fourier law. They integrate amplitude equations using power series;  $Ra_c$  was determined in a few cases as a function of the Biot number.

Hurle et al. [9] considered the case of a horizontal liquid layer set between two semi-infinite walls of equal thermal conductivity, different from that of the fluid. Gershuni et al. [10, 11] studied a more general case, but also less usual, in which the two semi-infinite walls have different thermal conductivities. They showed that the stability threshold is unchanged if the boundaries are interchanged and that an increase in thermal conductivity of the later involves a continuous increase in the critical Rayleigh number  $Ra_c$  and the corresponding wavenumber  $k_c$ . When both boundaries have the same thermal conductivity,  $Ra_c$  and  $k_c$  vary from, respectively, 720 and 0 to 1708 and 3.11, while the ratio of thermal conductivities decreases from infinity to zero. This variation can be easily understood when considering that a temperature fluctuation occurring in the liquid, close to a high conducting limiting plane, easily relaxes, whereas it can persist and distort the temperature distribution when the plane is nearly insulating. This distortion can lead to an instability of the fluid. As a consequence, the temperature gradient is small and the convective heat transfer too. The fluid layer organizes a pattern with small wavenumber.

All the theoretical works mentioned above were devoted to horizontal layers, infinitely extended in the

horizontal direction, whereas experiments are necessarily performed in finite vessels, where mechanical and thermal effects of lateral walls are always present, at least close to each wall. The questions of interest are then the following: what is the influence of the lateral walls, that of thermal properties and thicknesses of horizontal blocks of the vessel, on the value of the convective threshold?

Several authors considered the influence of confinement, i.e., of the lateral walls. It seems that the first investigator who considered a fully confined fluid was Davis [12, 13]. He chose perfectly conducting sidewalls in rectangular containers and used 'finite rolls' trial functions, with a Galerkin method which gives an upper limit for  $Ra_c$ . (The finite rolls are defined as convective cells having only two non-zero velocity components depending on the three spatial coordinates.) But this early theoretical work, criticized by Catton [14], was subsequently corrected by Davies-Jones [15]. He showed that, although the Davis finite rolls could not exist, they represent a good approximation of the true, three-dimensional solution. The reason for this is that the  $Ra_c$  problem is really a variation-problem to minimize a quadratic functional. Segel [16] used a multiple-scale perturbation analysis. Catton considered the case of a fluid confined above and below by rigid, perfectly conducting surfaces and laterally, by first perfectly conducting walls [14], then perfectly insulating [17] and finally arbitrary conducting ones [18]. Charlson and Sani [19] considered a finite cylindrical box, with good conducting top and bottom boundaries, whereas lateral walls were insulating or conducting. Qualitatively it can be concluded that lateral confinement is stabilizing for the fluid layer, but this effect is significant only for small aspect ratios ( $\Gamma_x$  and  $\Gamma_y < 2$ ). On the other hand,  $Ra_c$  is significantly smaller for insulating sidewalls than for conducting ones, especially for small aspect ratios. This result can be explained by the fact that the presence of lateral walls requires more work from the fluid, which has to overcome an additional viscous shear. This effect is reinforced if the lateral walls are good heat conductors because temperatures perturbations are more strongly damped in the neighbourhood of lateral walls. The latter requires an increase of the temperature gradient compared to the insulated lateral wall case. Stork and Müller [20] used a vessel with an upper 3 mm thick glass block and a lower 10 mm thick copper plate. They verified experimentally the onset of convection in small rectangular boxes with poorly conducting sidewalls. Their experimental values of  $Ra_c$  generally lie between the predicted values of the models for insulating and conducting sidewalls (with perfect heat conducting horizontal plates).

More recently, Luijckx and Platten [21] reconsidered the case of an infinite channel of rectangular cross section, with rigid perfect conducting horizontal boundaries and two rigid, perfectly insulated lateral walls. Amplitude-equation calculations of  $Ra_c$  lead to an asymptotic for-

mula for the critical Rayleigh number [22]. In this relation  $Ra_c$  depends only on the large aspect ratio of the container, provided the small dimension is at least a few roll diameters long and is independent of thermal properties of boundaries.

Although there has been extensive theoretical and experimental work on the problem of convective threshold in boxes, a question still remains to be answered: the initiation of convection in a fluid confined in a rectangular vessel with horizontal and vertical walls of arbitrary thermal conductivities and widths.

In further experimental studies, the following peculiar rectangular box will be used: the six vessel walls have finite thicknesses and thermal conductivities. Moreover, the sidewalls are not homogeneous and made up of two different materials. The goal of this paper is (i) to re-investigate the calculation of  $Ra_c$  for an infinite liquid layer set between horizontal blocks having finite thermal conductivities, (ii) to roughly estimate the value of  $Ra_c$  in the rectangular box described above.

The paper is organized as follows. In the next section (Section 2) a horizontal liquid layer is considered, infinitely extended in the horizontal direction, bounded by two rigid plates of different thicknesses and thermal conductivities. This problem is solved using the second variant of Bubnov–Galerkin method. The chosen trial function meets the boundary conditions and has sufficient freedom to look like the vertical component of the velocity being approximated. Critical Rayleigh number ( $Ra_c$ ) and wavenumber ( $k_c$ ) are calculated. The main results are presented in this section. Then the temperature field at the threshold, just before the starting of the convection is computed in Section 3, using a finite element model. Computations are also performed for boxes with two thermal conducting and two mean thermal conducting vertical walls, and for boxes with four mean conducting vertical walls. Section 4 describes the experimental procedure: experimental and calculated results are compared. In Section 5, some conclusions are gathered.

**2. The analytical model**

*2.1. Formulation*

A horizontal liquid layer of depth  $d$  is considered, infinitely extended in the horizontal direction. The liquid is bounded beneath and below by two rigid plates of different thicknesses  $d_u, d_l$  and different thermal conductivities  $\lambda_u, \lambda_l$  (the subscripts u and l stand, respectively, for the upper and the lower plates) (Fig. 1). The liquid obeys the Boussinesq conditions.

$\mathbf{V}$  and  $\Theta$  being, respectively, the velocity and the temperature perturbation from a uniform vertical tem-

perature gradient, for the steady solution, it is assumed the following expressions:

$$(\mathbf{V}, \Theta) = [u(z), v(z), w(z), \Theta(z)]f(x, y). \tag{1}$$

The coordinates  $x, y, z$ , the time  $t$ , the velocity and the temperature  $T$ , are scaled by  $d, d^2/\nu, \nu/d$  and  $\delta T$ , respectively, where  $\nu$  is the kinematic viscosity and  $\delta T$  the critical temperature difference. Applying a first order perturbation to a fluid which satisfies the Boussinesq approximation, the Navier–Stokes and energy equations lead to, respectively:

$$(D^2 - k^2)^2 w - Ra \Theta k^2 = 0 \tag{2}$$

$$(D^2 - k^2)\Theta + w = 0 \tag{3}$$

where  $Ra = \alpha g \delta T d^3 / \nu \kappa$  is the Rayleigh number,  $\alpha$  is the coefficient of thermal expansion of the liquid,  $g$  is the gravity,  $\delta T$  is the temperature difference between the limiting horizontal surfaces,  $\kappa$  is the thermal diffusivity and  $D = d/dz$ .

The mechanical boundary conditions correspond to rigid plates and to no slip conditions:

$$z = \pm 1/2 \quad w = Dw = 0. \tag{4}$$

For thermal boundary conditions, a constant and uniform temperature is assumed over the outer surface of each plate (the surfaces in contact with the thermostated baths):

$$z = -(1/2 + \delta_l) \quad \Theta = \Theta_l = 0 \tag{5}$$

$$z = (1/2 + \delta_u) \quad \Theta = \Theta_u = 0 \tag{6}$$

where  $\delta_i = d_i/d$  ( $i = u, l$ )

The continuity condition for temperature and heat flux are written:

$$z = -1/2 \quad \Theta = \Theta_l \quad r_l D\Theta = D\Theta_l \tag{7}$$

$$z = +1/2 \quad \Theta = \Theta_u \quad r_u D\Theta = D\Theta_u \tag{8}$$

with  $r_i = \lambda/\lambda_i$  ( $i = u, l$ ),  $\lambda$  being the thermal conductivity of the fluid.

*2.2. Method of solution*

To solve equations (2)–(6), it is necessary to know  $\Theta_u$  and  $D\Theta_u$ . In the upper plate, the steady temperature field is considered, which satisfies Laplace’s equation  $\Delta\Theta_u = 0$ . A general solution is:

$$\Theta_u = A_u \exp(kz) + B_u \exp(-kz). \tag{9}$$

Taking into account equations (6) and (8) leads to:

$$\Theta_u = A_u [1 - \exp(2k\delta_u)] \exp\left(\frac{k}{2}\right) \tag{10}$$

$$r_u D\Theta_u = A_u [1 + \exp(2k\delta_u)] k \exp\left(\frac{k}{2}\right). \tag{11}$$

Combining equations (10) and (11) with:

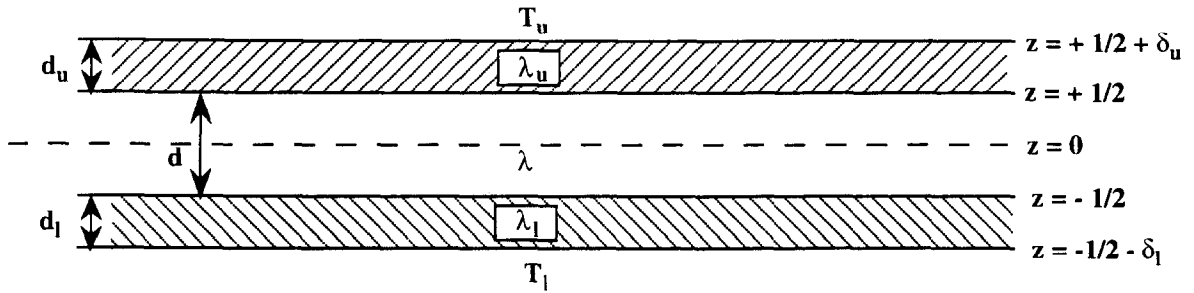


Fig. 1. Boundaries in Rayleigh–Bénard convection.

$$\beta_u = \frac{1}{r_u \tanh(k\delta_u)} \quad (12)$$

it is finally obtained :

$$\text{on } z = 1/2 \quad D\Theta_u = -\Theta_u k\beta_u \quad (13)$$

with a similar equation on  $z = -1/2$  :

$$D\Theta_l = \Theta_l k\beta_l \quad \text{with } \beta_l = \frac{1}{r_l \tanh(k\delta_l)}. \quad (14)$$

The system of equations (2)–(8) is solved using the Bubnov–Galerkin method [11]. Somewhat arbitrarily, but primarily for reasons of simplicity, of satisfaction of the boundary conditions and the velocity profile being approximated, the following function is chosen :

$$w = E(1 + \cos 2\pi z) + F(1 - \cos 4\pi z). \quad (15)$$

Then substituting (15) into (2) and taking into account boundary conditions, the following general solution for  $\Theta$  is obtained :

$$\Theta = E\Theta_1 + F\Theta_2 \quad (16)$$

with

$$\Theta_1 = \phi_1 \text{sh}(kz) + \xi_1 \text{ch}(kz) + (k^{-2} + \gamma_1^{-1} \cos 2\pi z) \quad (17)$$

$$\Theta_2 = \phi_2 \text{sh}(kz) + \xi_2 \text{ch}(kz) + (k^{-2} - \gamma_2^{-1} \cos 4\pi z) \quad (18)$$

and

$$\xi_1 = + \frac{4\pi^2}{k^2 \gamma_1} \xi, \quad \xi_2 = + \frac{16\pi^2}{k^2 \gamma_2} \xi$$

$$\phi_1 = \frac{4\pi^2}{\gamma_1 k^2} \phi, \quad \phi_2 = \frac{16\pi^2}{\gamma_2 k^2} \phi$$

$$\xi = - \frac{(\beta_u + \beta_l) \text{ch} \frac{k}{2} + 2\beta_u \beta_l \text{sh} \frac{k}{2}}{G}, \quad \phi = \frac{(\beta_l - \beta_u) \text{sh} \frac{k}{2}}{G}$$

$$G = (1 + \beta_u \beta_l) \text{sh} k + (\beta_u + \beta_l) \text{ch} k$$

$$\gamma_1 = k^2 + 4\pi^2, \quad \gamma_2 = k^2 + 16\pi^2. \quad (19)$$

Since  $w$  and  $\Theta$  must satisfy equation (1), it is required that

$$E(k^4 + \gamma_1^2 \cos 2\pi z - Ra \Theta_1 k^2) + F(k^4 - \gamma_2^2 \cos 4\pi z - Ra \Theta_2 k^2) = 0. \quad (20)$$

Multiplying (20) by  $(1 + \cos 2\pi z)$  and integrating with respect to  $z$  from  $-1/2$  to  $+1/2$ , then doing the same with  $(1 - \cos 4\pi z)$ , a formula for the Rayleigh number is finally obtained :

$$Ra = \frac{-(I_4 J_1 + I_1 J_4 - 2I_2 J_2)}{2(J_1 J_4 - J_2^2)} \pm \frac{[(I_4 J_1 + I_1 J_4 - 2I_2 J_2)^2 - 4(I_1 I_4 - I_2^2)(J_1 J_4 - J_2^2)]^{0.5}}{2(J_1 J_4 - J_2^2)} \quad (21)$$

with :

$$I_1 = k^4 + \frac{\gamma_1^2}{2}, \quad I_2 = I_3 = k^4, \quad I_4 = k^4 + \frac{\gamma_2^2}{2}$$

$$J_1 = - \left[ 1 + \frac{k^2}{2\gamma_1} + 2 \frac{\xi}{k} \left( \frac{4\pi^2}{\gamma_1} \right)^2 \text{sh} \frac{k}{2} \right], \quad (22)$$

$$J_2 = J_3 = - \left[ 1 + 2 \frac{\xi}{k} \frac{64\pi^4}{\gamma_1 \gamma_2} \text{sh} \frac{k}{2} \right]$$

$$J_4 = - \left[ 1 + \frac{k^2}{2\gamma_2} + \frac{2\xi}{k} \left( \frac{16\pi^2}{\gamma_2} \right)^2 \text{sh} \frac{k}{2} \right].$$

The relation (21) provides the Rayleigh number of the fundamental instability mode as a function of five parameters: the wavenumber  $k$ , the conductivity ratios  $r_u$  and  $r_l$ , the thickness ratios  $\delta_u$  and  $\delta_l$ . After fixing last four parameters,  $Ra$  is calculated as  $k$  varies from 0 to infinity. The critical value  $Ra_c$  corresponds to the minimum of  $Ra$ .

### 2.3. Results

From equations (21) and (22) it is easily seen that  $Ra_c$  is a symmetric function in terms of  $r_u$  and  $r_l$ ,  $\delta_u$  and  $\delta_l$  i.e.,

$$Ra(r_u, r_l) = Ra(r_l, r_u) \quad (23)$$

$$Ra(\delta_u, \delta_l) = Ra(\delta_l, \delta_u) \quad (24)$$

thus, the threshold is unchanged if the thermal conductivities and/or the thicknesses are interchanged. In the following, when  $\delta$  (or  $r$ ) is used without subscript, it

denotes that  $\delta = \delta_u = \delta_l$  (or  $r = r_u = r_l$ ). Some interesting special cases are first examined.

2.3.1. Both blocks are perfect heat conductors ( $r \approx 4 \cdot 10^{-6}$ )

$Ra_c$  and  $k_c$  are independent of  $\delta$ . Obviously, when the horizontal blocks are perfect conductors, their thickness has no influence on the threshold. The value  $Ra_c = 1731$  is greater than the exact value  $Ra_c = 1708$  [4, 10, 11], but the difference is only 1.3%.

2.3.2. Both blocks are perfect heat insulators ( $r \approx 4 \cdot 10^6$ )

Likewise, whatever the thickness of blocks, there is a unique critical value for  $Ra_c$ . The founded value  $Ra_c = 734$  is larger than the exact one,  $Ra_c = 720$  [10, 11]; the difference reaches 1.9%.

2.3.3. Influence of  $r$  and  $\delta$  with identical blocks

Hurle et al. [9], Reid and Harris [3], Gershouni et al. [10, 11], calculated  $Ra_c$  for two semi infinite walls. Figure 2 shows that our results agree with that of Gershouni et al. [11] to 1% for  $\delta > 1$ . For the values  $\delta = 1$  and  $10^{-1} < r < 10^2$ , which are of practical interest (these cor-

respond to real boxes), the difference between the two results can reach 20%. For  $k_c$  the difference can be larger: it is 100% when  $\delta = 0.1$  and  $r = 0.4$  (Fig. 3).

In conclusion, the approximation of precited authors is valuable only for limiting cases:  $r$  very small or very large, and of course, when the thickness of the two limiting horizontal plates is much larger than the depth of the layer; the precise knowledge of  $Ra_c$  and  $k_c$  for a real case ( $\delta < 10$  and  $r$  finite) requires a special calculation. For instance, for a silicone oil ( $d = 1$  cm and  $\lambda = 0.16$  W m K<sup>-1</sup>) set between two blocks ( $d_i = 0.3$  cm and  $\lambda_i = 0.22$  W m K<sup>-1</sup>) the calculation, for  $r = 1.375$  and  $\delta = 0.3$ , gives  $Ra_c = 1318$  and  $k_c = 2.60$ , whereas the approximation previously cited provides  $Ra_c = 1212$  and  $k_c = 2.07$ . The differences are respectively 9 and 26%.

2.3.4. Influence of  $r$  and  $\delta$  when the blocks are different.

The variation of  $Ra_c$  as a function of  $r_l$  (or  $r_u$ ) for various  $r_u$  ( $r_l$ ) is displayed in Figs. 4 and 5 for, respectively,  $\delta = 100$  and for  $\delta = 0.1$ . As already pointed out by Gershouni et al. [10, 11],  $Ra_c$  ( $k_c^{-1}$ ) decreases when the thermal conductivity of a bounding surface decreases. When the thermal conductivity of the first block decreases from infinity to zero,  $Ra_c$  decreases from 1731

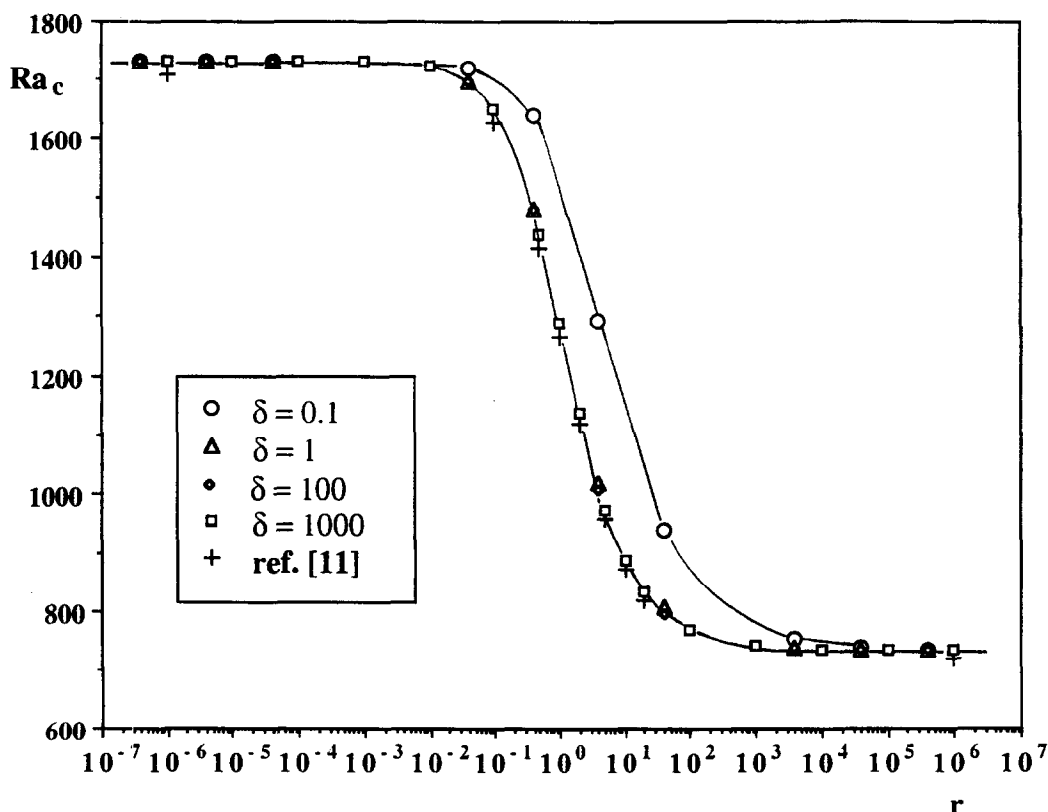


Fig. 2. Critical Rayleigh number, as a function of the ratio  $r = \lambda_{liquid}/\lambda_{block}$  of the thermal conductivities for various thickness blocks.

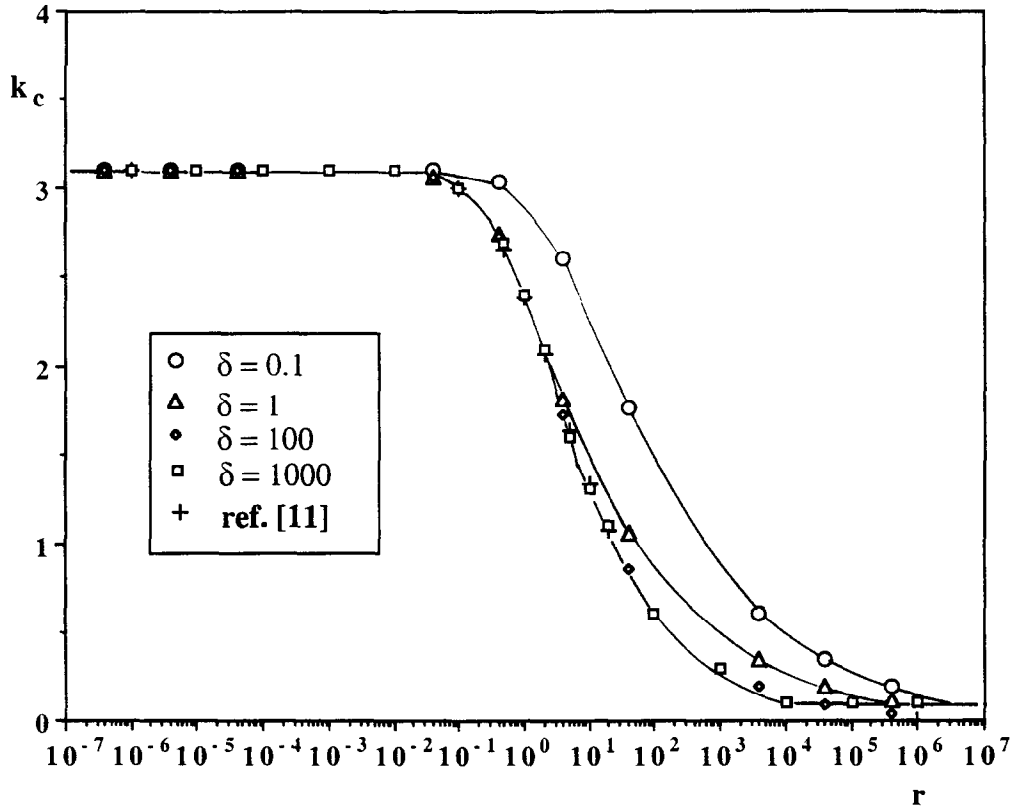


Fig. 3. Critical wavenumber as a function of the ratio  $r = \lambda_{\text{liquid}}/\lambda_{\text{block}}$  of the thermal conductivities for various thickness blocks.

to 1326 when the second block is a perfect thermal conductor, whereas it varies from 1326 to 734 when it is a perfect insulator. Variations of  $Ra_c$  ( $k_c^{-1}$ ) as a function of  $\delta_u$  ( $\delta_l$ ), for various  $\delta_l$  ( $\delta_u$ ) for fixed  $r$ , display the same behaviour (indeed equations (12) and (14) show that  $r_l$  and  $\delta_l$  have similar part on  $\beta$ ).

### 3. Conductive state in a finite vessel

To estimate the influence of the thermal properties of side walls on the onset of convection in a finite rectangular box, in view of new experiments to be developed in the future, the temperature field was calculated in the motionless liquid and in the vessel walls. The liquid under consideration was a silicon oil Rhodorsil 47V100 (the liquid used in our experiments on Rayleigh–Bénard convection). The critical value, for an infinite layer,  $Ra_c = 1318$  corresponds to  $\delta T_c = 1.65^\circ\text{C}$ . Calculations were performed for a vertical temperature difference  $\delta T = 1.6^\circ\text{C}$ . Such a study provided the temperature field near the threshold, and some insight into the influence of

the confinement, the presence of inhomogeneities in the sidewalls, as well as the heat transfers.

#### 3.1. Vessels

The vessel under study is a rectangular cavity ( $1 \times 3 \times 12 \text{ cm}^3$ ), filled with silicon oil Rhodorsil 47V100 (Prandtl number = 880 at  $25^\circ\text{C}$ ) (Fig. 6). The walls are made of transparent polycarbonate, which has approximately the same thermal conductivity ( $0.22 \text{ W m K}^{-1}$ ) as the silicon oil ( $0.16 \text{ W m K}^{-1}$ ). Therefore, convection occurs in a box with moderate aspect ratios ( $\Gamma_x = 12$ ,  $\Gamma_y = 3$ ), between moderately heat conducting walls ( $r = 0.73$ ) and finite horizontal blocks ( $\delta = 0.3$ ). The outside surfaces of blocks  $C$  and  $C'$  are in contact respectively with streams of warm and cold water, maintained at fixed temperatures (Rayleigh–Bénard conditions). In each of the two small lateral walls  $A$  and  $A'$ , a horizontal parallelepiped ( $5 \times 0.5 \times 0.6 \text{ cm}^3$ ) made of copper is inset. The thickness of  $A$  and  $A'$  is 1 cm, that of  $C$  and  $C'$  is 0.3 cm, whereas that of  $B$  and  $B'$  (the other two lateral walls not shown in Fig. 6) is 1 cm.

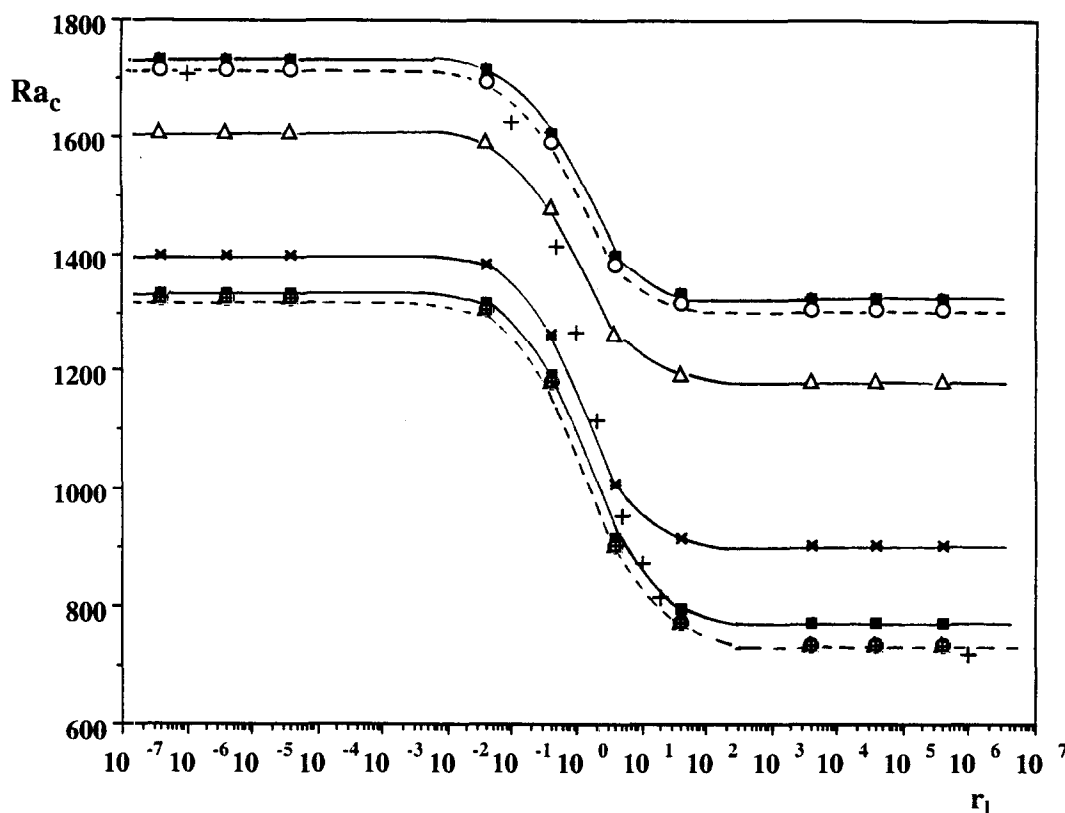


Fig. 4. Critical Rayleigh number as a function of the relative thermal conductivity of one block, for various relative thermal conductivities of the second block. Relative thickness of each block:  $\delta = 100$ .  $r_u = \square 4 \cdot 10^{-7}$ ,  $\diamond 4 \cdot 10^{-6}$ ,  $\times 4 \cdot 10^{-5}$ ,  $\circ 4 \cdot 10^{-2}$ ,  $\triangle 4 \cdot 10^{-1}$ ,  $*$   $4 \cdot 10^{+1}$ ,  $\bullet 4 \cdot 10^{+3}$ ,  $\blacktriangle 4 \cdot 10^{+4}$ ,  $\boxplus 4 \cdot 10^{+5}$ , + ref. [11].

Two homogeneous vessels were also considered, with same geometrical characteristics, one made of copper, the other of polycarbonate.

### 3.2. Physical model and hypothesis

The steady-state thermal behaviour of the system is considered, just before the onset of convection, i.e. before the onset of the main Rayleigh–Bénard type cellular flow. The study is carried out with a three-dimensional (3-D) model, with appropriate geometry and boundary conditions.

The whole system, that is the motionless oil contained in the box, the six polycarbonate vessel walls and the copper elements, is included in the formulation of the field problem. The thermal interaction between the polycarbonate surface and the water flows is approximated by specifying a constant temperature over the upper and lower walls.

The vertical sidewalls of the box are considered initially as adiabatic. A second series of calculations is then performed, using natural convection heat transfer

coefficients between the sidewalls and the surrounding atmosphere.

Because of the symmetry of geometry and physical loadings, the 3-D domain of the computation is taken to be only one quarter of the box.

### 3.3. Finite element model

The solution domain is classically divided into non-overlapping 20-node (quadratic interpolation) hexahedral finite elements and the continuous temperature field, within each element, expressed in terms of the 20 unknown nodal values of the same element [23].

The convective heat transfer across the vertical boundaries of interest is involved by using special 8-node planar finite elements [24]. These elements have full compatibility with the faces of the 246 20-node elements used to model the three media: oil, copper and polycarbonate.

### 3.4. Calculations

They were performed with use of the MEF/MOSAIC\* code in three vessels: the box described above ( $VE_{pc}$ ),

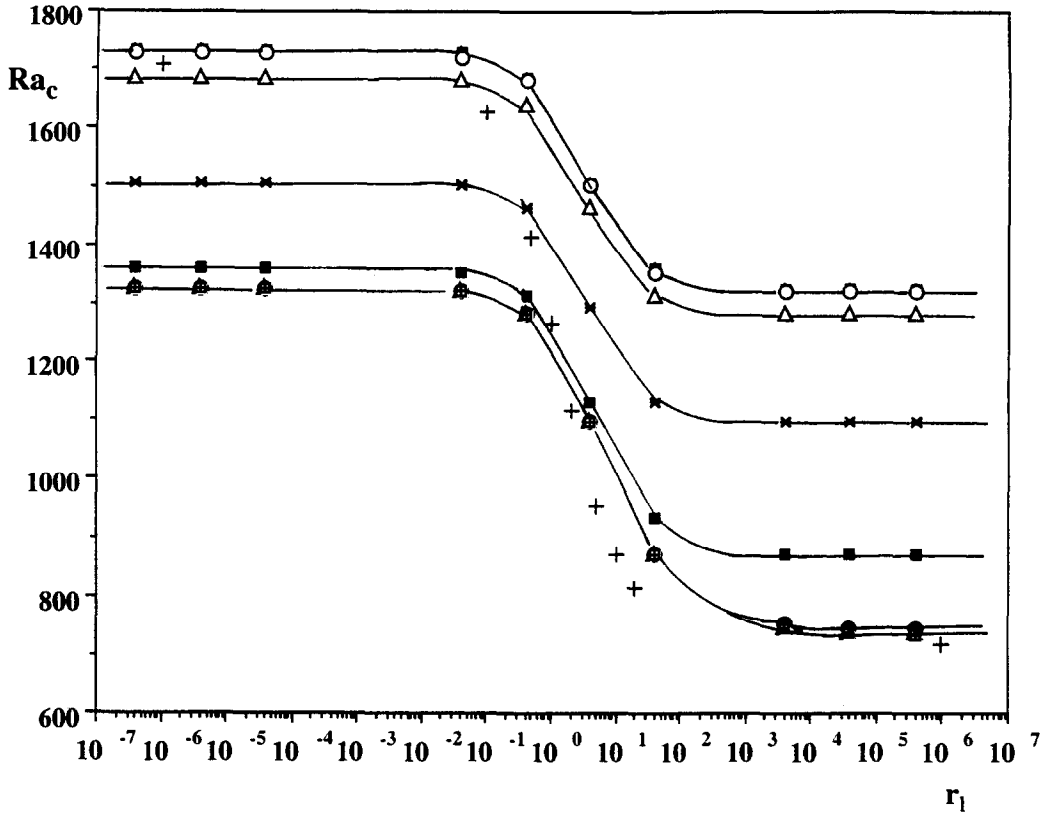


Fig. 5. Critical Rayleigh number as a function of the relative thermal conductivity of one block, for various relative thermal conductivities of the second block. Relative thickness of each block:  $\delta = 0.1$ .  $r_w = \square 4 \cdot 10^{-7}$ ,  $\diamond 4 \cdot 10^{-6}$ ,  $\times 4 \cdot 10^{-5}$ ,  $\circ 4 \cdot 10^{-2}$ ,  $\triangle 4 \cdot 10^{-1}$ ,  $* 4$ ,  $\blacksquare 4 \cdot 10^1$ ,  $\bullet 4 \cdot 10^3$ ,  $\blacktriangle 4 \cdot 10^4$ ,  $\boxplus 4 \cdot 10^5$  + ref. [11].

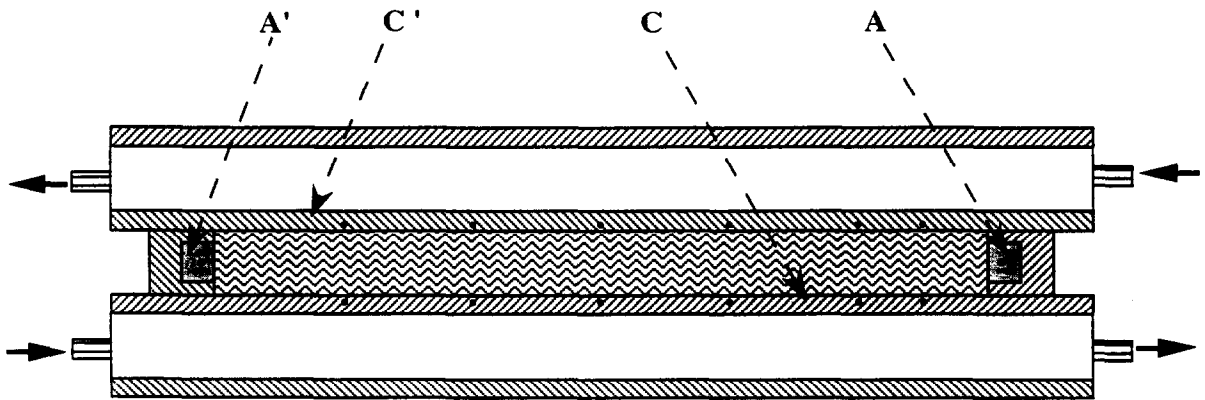


Fig. 6. Schematic section of the vessel. The fourteen black points in C, C', A and A' point out the thermocouples.

and, for comparison, two homogeneous boxes having the same size, but made up of polycarboxylate ( $VE_p$ ) or copper ( $VE_c$ ). The mean temperature of the liquid was  $22.8^\circ\text{C}$ . For each box, adiabatic or conducting sidewalls were considered. For the last case, the convective

exchange coefficient ' $h$ ' between lateral walls and the atmosphere was given by the mean-value formula :

$$h = 3.85(T_w - T_\infty)^{1/4} \tag{25}$$

with  $T_w$  and  $T_\infty$ , respectively, the wall and the atmosphere



temperatures. Calculations were performed with  $T_\infty = -3, 25$  or  $47^\circ\text{C}$ .

**3.5. Results**

Figures 7 and 8 show the isotherms in the central vertical longitudinal plane (plane LP) or in the central vertical transverse plane (plane TP) of the vessel.

**3.5.1. Adiabatic sidewalls (Fig. 7)**

The copper rods strongly disturb the distribution of isotherms in their neighbourhood (Fig. 7(a)); however the rod is essentially isothermal elsewhere. This non uniform temperature gradient in the liquid is the origin of a convective roll existing close to wall *A*, even for small  $\delta T$ . Figure 7(b) and (c), show the isotherms in  $VE_c$  or  $VE_p$ . In both cases the lateral walls weakly modify the temperature field. Let us define the thermal influence length (TIL) as the length, measured from the vessel wall, where the temperature field is non uniform. This TIL is the same for  $VE_c$  or  $VE_p$  (0.6 cm), whereas it is 1.1 cm for our  $VE_{pc}$ . In the transverse plane, the isotherms are obviously alike for the  $VE_{pc}$  and  $VE_p$ , as well as the TIL.

In conclusion, the heterogeneous wall ( $VE_{pc}$ ) disturbs the isotherms more than the homogeneous walls ( $VE_c$

and  $VE_p$ ), as expected. For the three cases, there is a decrease of  $\delta T$ , along the wall *A*, in comparison to that in the central part of the box. The corresponding decrease of *Ra* is 33% for  $VE_{pc}$  and  $VE_c$ , and only 15% for  $VE_p$ . But, close to the vessel wall, the vertical temperature gradient is constant for  $VE_c$  and  $VE_p$ , whereas for  $VE_{pc}$ , it strongly varies in front of the polycarbonate and is about zero in front of the copper element (which is an isotherm surface to less than  $0.1^\circ\text{C}$ ). That means that the walls have a stabilizing effect on the liquid in  $VE_c$  and  $VE_p$ , and a destabilizing one in  $VE_{pc}$ .

It is noteworthy that the hypothesis of adiabaticity is a more or less justified approximation in a real case. Indeed it is approximately realized when the external temperature is equal to the average temperature of the fluid, but, necessarily in this case heat transfer occurs from outside to the fluid in the upper part of the vessel; it is the reverse in the lower part. Herein hypothesis is justifiable since  $\delta T$  is small.

**3.5.2. Weak heat exchange with the surrounding atmosphere**

When the outside temperature is  $25^\circ\text{C}$ , i.e.  $2.2^\circ\text{C}$  more than that of the liquid, it can be observed that the temperature field is not significantly modified in the liquid

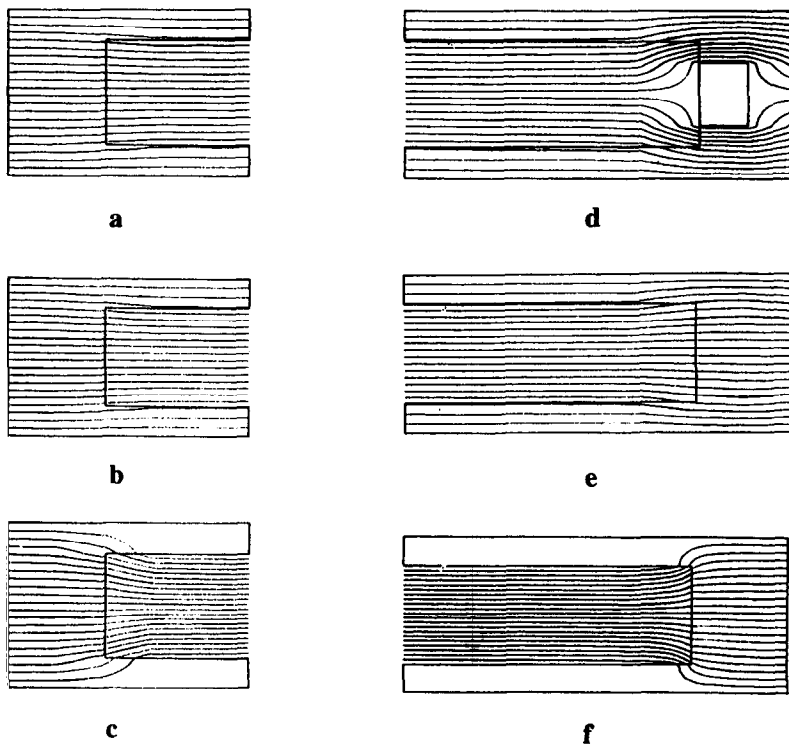


Fig. 7. Twenty isotherms for adiabatic sidewalls, in the transverse plane (a, b, c) and in the longitudinal plane (d, e, f), for the various vessels  $VE_{pc}$  (a, d),  $VE_p$  (b,e),  $VE_c$  (c, f).  $T_u = 22^\circ\text{C}$ ,  $T_l = 24.3^\circ\text{C}$  ( $VE_p, VE_{pc}$ ) and  $T_l = 23.6^\circ\text{C}$  ( $VE_c$ ).

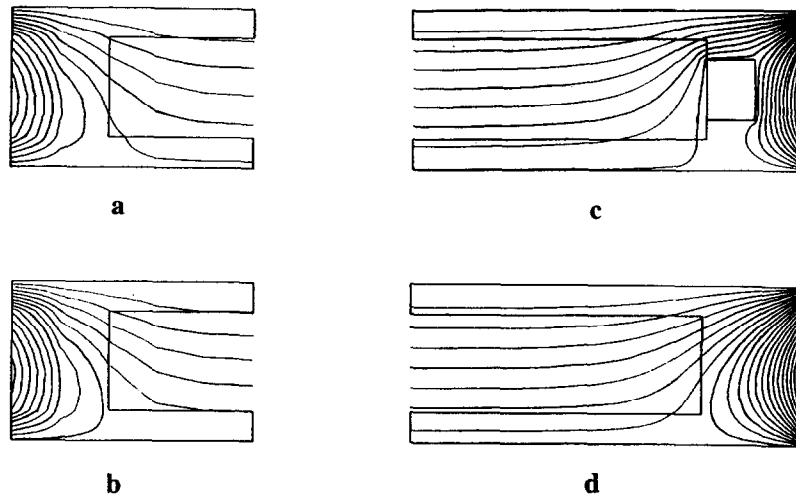


Fig. 8. Twenty isotherms for strong convective thermal exchange with the atmosphere ( $T_\infty = 47^\circ\text{C}$ ), in the transverse plane (a, b) and in the longitudinal plane (c, d) for the vessels  $VE_{pc}$  (a, c) and  $VE_p$  (b, d), with  $T_u = 22^\circ\text{C}$  and  $T_l = 24.3^\circ\text{C}$ .

layer. The position of the isotherms is not modified in the copper box and is only weakly perturbed in the vessel wall, in the neighbourhood of the external surface. The vertical displacement of an isotherm is about 1.3 mm in  $VE_p$ , 1.5 mm in  $VE_{pc}$ , whereas the isotherms remain at the same position in  $VE_c$ . The TIL is slightly increased, it is 1.3 cm instead of 1.1 cm. In the transverse plane, the behaviours are similar.

### 3.5.3. Strong heat exchange with the surrounding atmosphere (Fig. 8)

The important heat transfers between the vessel and the surrounding atmosphere strongly displace, as expected, the isotherms in the neighbourhood of the walls and inside the walls themselves. The TIL reaches 2.5 cm in the real box and 2.1 cm in the polycarbonate vessel, but there is no apparent change for the copper container. It is similar in the transverse plane. Close to the walls, the temperature field is strongly non uniform, a convective roll along the wall can exist whereas in the central part of the vessel, the temperature gradient is constant. In this region the convective Bénard rolls can appear only when the threshold is reached and if the aspect ratios  $\Gamma_x$  and  $\Gamma_y$  are large enough.

The thermal influence of walls was considered, but the convective threshold also (overall) depends on their mechanical influence. Many calculations on the critical Rayleigh number in vessels with horizontal conducting surfaces have been performed by various authors with 'slippery' and impermeable or 'non slippery' sidewalls. The second condition, the only realistic one, exhibits a noticeable increase in comparison to the first one, exhibiting the importance of mechanical influence of the lateral confinement. To determine the critical Rayleigh

number in our vessel, it is necessary to conduct experiments.

## 4. Experiments

### 4.1. Experimental procedures

The vessel is described above. The temperatures on the faces of  $C$  and  $C'$ , in contact with the liquid under consideration and in the copper parts of  $A$  and  $A'$ , were measured with fourteen thermocouples (diameter = 0.5 mm) (Fig. 6). Silicon oils, of viscosities 5 and 10 Stokes at  $25^\circ\text{C}$ , were used for the determination of  $Ra_c$ . Indeed, increasing  $\nu$  increases the critical temperature difference  $\delta T_c$ , and decreases the uncertainty in  $Ra_c$ .

The flows were visualized in vertical and horizontal planes by using a plane laser beam and small aluminium flakes dispersed in the liquid. For the determination of the critical temperature difference, two independent methods were used: (i) visualisation of the initial convection by means of the aluminium flakes, made visible when illuminated by the laser beam. They were observed with a microscope using a black background. A displacement of the order of  $0.5 \mu\text{m s}^{-1}$  could be detected; (ii) recording the temperature as a function of time. The onset of convection corresponded to a kink in the temperature vs. time plot.

Experiments were performed with a slow heating rate ( $1^\circ\text{C}$  per hour) and for the adiabatic case, i.e., for a mean liquid temperature equal to that of the surrounding atmosphere ( $23^\circ\text{C}$ ).

#### 4.1.1. Estimation of error in $Ra_c$

The  $\alpha$  and  $\kappa$  quantities are given in the manufacturer catalogue (Rhône Poulenc Rhodorsil Silicones). The viscosity is calculated at the average temperature  $T_m = (T_l + T_u)/2$  ( $T_l$  and  $T_u$  are the temperatures, respectively, at the lower and the upper surfaces of the liquid layer). The errors in  $\alpha$ ,  $\nu$  and  $\kappa$  are assumed to be, respectively, 1, 0.5 and 1%. The error in the depth layer is 0.5%. After calibration of the thermocouples, the error in the critical temperature difference was estimated to  $\pm 0.05^\circ\text{C}$ . Using high viscosity oils increases  $\delta T_c$  and decreases the relative uncertainty: it was about  $6 \cdot 10^{-3}$  and  $3 \cdot 10^{-3}$  for oils of 5 and 10 Stokes, respectively. The major cause of error in the measurement of  $Ra_c$  is the sensitivity in the detection of the threshold. After numerous tries, it was estimated to be to  $\pm 0.1^\circ\text{C}$ . Thus, the uncertainty in the critical Rayleigh number may contain errors up to a maximum of 6%. This value must be considered as a maximum because the various errors may at least partly compensate each other.

#### 4.2. Results

The two methods mentioned above provided consistent results for both oils in almost adiabatic lateral wall case. Results are tabulated in Table 1. For each temperature five measurements were performed. The corresponding mean  $Ra_c$  is 1420, which is close to the value calculated for an infinite layer ( $Ra_c = 1312$ ). The difference (8.2%) is larger than the estimated maximum uncertainty (6%).

It is noteworthy that the critical Rayleigh number in a box is larger than in an infinite layer. This is in agreement with the results reported in the Introduction, but for different vessels, i.e. the two limiting horizontal surfaces were assumed to be perfectly conducting whereas, in the box under consideration, they have a finite thermal conductivity. If the Catton [17, 18] results are transposed to this case, the variation of  $Ra_c$  is of the order of 6–7%; on the other hand, the formula of Walden et al. [25],

appropriate for a rectangular box of aspect ratios  $10 \times 5$  with horizontal heat conducting plates, predicts a variation of about 5% for  $Ra_c$ . All these results, although established for different vessels, are in agreement with our measurements.

#### 5. Conclusion

The influence of the thermal conductivities and thicknesses of horizontal plates in a box, on  $Ra_c$  and  $k_c$ , is important for small thicknesses and intermediate conductivities. The influence of lateral walls in a finite box is noticeable for small aspect ratios, as pointed out by Catton, but for different thermal and geometrical conditions. In fact it is very important for very small aspect ratios only. That seems to be a quite general result. The sidewalls have a double effect: (i) they increase the  $\delta T$  in the influence zone and they damp the thermal perturbations. As shown by many authors, this effect is more pronounced with conducting walls than with isolated ones; (ii) they damp the velocity perturbations. The effect of the lateral walls is doubly stabilizing, and thus follows an increase in  $Ra_c$ .

#### Acknowledgement

We thank R. L. Sani for many comments and valuable discussions.

#### References

- [1] Bénard H. Les tourbillons cellulaires dans une nappe liquide propageant de la chaleur par convection en régime permanent Paris: Thèse Université de Paris, 1900.
- [2] Rayleigh L. On convection currents in a horizontal layer of fluid when the higher temperature is on the under side. *Philos Mag* 1916;32:529–43.
- [3] Reid WH, Harris DL. Streamlines in Bénard convection cells. *Phys Fluids* 1959;2:716–27.
- [4] Chandrasekhar S. Hydrodynamics and hydromagnetic stability. London, U.K.: Clarendon Press, Oxford University, 1961. p. 43.
- [5] Koschmieder EL. Bénard cells and Taylor vortices. Batchelor ed., Cambridge University Press, 1993.
- [6] Jeffreys H. The stability of a layer heated from below. *Phil Mag* 1926;2:833–44.
- [7] Sani RL. Convective instability, Ph.D. thesis in Chemical Engineering, University of Minnesota, 1963.
- [8] Sparrow EM, Goldstein RJ, Jonsson VH. Thermal instability in a horizontal fluid layer: effect of boundaries conditions and nonlinear temperature profile. *J Fluid Mech* 1964;18:513–28.
- [9] Hurlle DT, Jakeman E, Pike ER. On the solution of Bénard problem with boundaries of finite conductivities. *Proc Roy Soc A* 1967;296:469–75.

Table 1  
Critical Rayleigh number and critical temperature difference measured for various mean temperatures  $T_m$  of the liquid and of the atmosphere for two silicone oils

Oil (Stokes)	$T_m = T_\infty$ ( $^\circ\text{C}$ )	$\delta T_c$ ( $^\circ\text{C}$ )	$Ra_c$
5	20	9.1	1416
	25	8.65	1431
	27	8.35	1405
10	20	19.25	1422
	25	17.2	1412
	30	15.75	1432

- [10] Gershuni GZ, Zhukhovitskii EM, Semakin IG. On convective instability in a horizontal fluid layer separating walls of different conductivity. *Uchen Zap Perm Univ* 1967;248:18–29. *Gidrodinamika*.
- [11] Gershuni GZ, Zhukhovitskii EM. Convective stability of incompressible fluids. Jerusalem: Israel Program for Scientific Translations, 1976. p. 32.
- [12] Davis SH. Convection in a box: linear theory. *J Fluid Mech* 1967;30:465–78.
- [13] Davis SH. Convection in a box: on the dependence of preferred wave-number upon the Rayleigh number at finite amplitude. *J Fluid Mech* 1968;32:619–24.
- [14] Catton I. Convection in a closed rectangular region: the onset of motion. *Journal of Applied Mechanics* 1970;C92:186–8.
- [15] Davies-Jones RP. Thermal convection in an infinite channel with no slip side-walls. *J Fluid Mech* 1970;44(4):695–704.
- [16] Segel LA. Distant side-wall cause slow amplitude modulation of cellular convection. *J Fluid Mech* 1969;38:203–24.
- [17] Catton I. The effect of insulating vertical walls on the onset of motion in a fluid heated from below. *Int J Heat Mass Transfer* 1972;15A:665–72.
- [18] Catton I. Effect of wall conduction on the stability of a fluid in a rectangular region heated from below. *J Heat Transfer* 1972;94C:446–52.
- [19] Charlson GS, Sani RL. Thermoconvective instability in a bounded cylindrical fluid layer. *Int J Heat Mass Transfer* 1970;13:479–96.
- [20] Stork K, Müller U. Convection in boxes: experiments. *J Fluid Mech* 1972;54:599–611.
- [21] Luijckx JM, Platten JK. On the onset of free convection in a rectangular channel. *J Non-Equilib Thermodyn* 1981;61:141–57.
- [22] Greenside HS, Coughran WM. Non linear pattern formation near the onset of Rayleigh–Bénard convection. *Phys Rev A* 1984;30:398–428.
- [23] Huebner KN, Thornton EA. *The finite element method for engineers*. John Wiley and Sons, 1982. pp. 406–435.
- [24] Dhatt G, Touzot G. Une présentation de la méthode des éléments finis, Maloine S. A. (ed), p. 123.
- [25] Walden RW, Kolodner P, Passner A, Surko CM. Heat transport by parallel-roll convection in a rectangular container. *J Fluid Mech* 1987;185:205–34.